

Synthesis, Spectral Characterization and Fluorescent Assessment of 1,3,5-Triaryl-2-pyrazoline Derivatives: Experimental and Theoretical Studies

Mohammad M. Ibrahim¹ · Mahmoud Al-Refai¹ · Khurshid Ayub² · Basem F. Ali^{1,3}

Received: 22 March 2016 / Accepted: 9 May 2016 / Published online: 24 May 2016
© Springer Science+Business Media New York 2016

Abstract Two new pyrazoline derivatives, namely 5-(4-bromophenyl)-3-(5-chlorothiophen-2-yl)-1-phenyl-4,5-dihydro-1*H*-pyrazole (**3**) and 5-(4-bromophenyl)-3-(2,5-dichlorothiophen-3-yl)-1-phenyl-4,5-dihydro-1*H*-pyrazole (**4**) have been synthesized and characterized based on their spectral (IR, ¹H and ¹³C NMR and MS) data and microanalysis. The fluorescence properties of **3** and **4** were studied by UV–Vis and emission spectroscopy. For compound **3**, a fluorescence emission was observed in the blue region of the visible spectrum. The effect of different solvents on fluorescence was also investigated. Density Functional Theory calculations have also been performed to gain insight into geometric, electronic and spectroscopic properties of the pyrazoline derivatives. Both structures are analysed and compared in order to rationalize the different behaviour in **3** and **4**.

Keywords Pyrazolines · Chalcone · Spectral characterization · DFT calculations · Fluorescence

Introduction

Pyrazolines are very important five-membered heterocycles since they are reported to have a wide spectrum of potential pharmacological activities, such as antimicrobial [1, 2] anticancer [3–5], anti-inflammatory [6, 7], antioxidant [8, 9], antidepressant [10, 11], and many other activities [12]. The pyrazoline heterocycles are known as intramolecular charge transfer compounds of immense importance [13, 14]. Due to their fluorescent properties, they are widely used as hole-transport materials in the electrophotography and electroluminescence [14–16]. Of particular interest are 1,3,5-triaryl-2-pyrazolines which are considered as an important class of conjugated nitrogen-containing fluorescent compounds with blue emission with very high quantum yield [17–20]. Moreover, organic electroluminescent compounds find application in various display devices mainly due to their high luminous efficiency, low cost, wide range of emission colors via specialized molecular design of organic compounds, and easy processing [21, 22]. 1,3,5-Triaryl-2-pyrazolines are also utilized as optical brightening agents [23], fluorescent switches [24], and as probes in many chemosensors [25].

In this work, we reported the synthesis of two new 1,3,5-triaryl-2-pyrazolines by adopting recent literature protocol [26], in which the appropriate acetylthiophene underwent Claisen-Schmidt condensation with the corresponding aldehydes in the presence of catalytic amount of KOH to afford the corresponding chalcones in high yield. Treatment of the chalcones with phenylhydrazine gave the pyrazoline derivatives **3** and **4** as the sole products in moderate yield. Characterization, Density Functional Theory (DFT) optimization of the structures and calculated spectral data along with the study of fluorescent properties of new pyrazoline compounds is also investigated.

✉ Basem F. Ali
bfali@kfu.edu.sa; bfali@aabu.edu.jo

¹ Department of Chemistry, Al al-Bayt University, Mafrq 25113, Jordan

² Department of Chemistry, COMSATS Institute of Information Technology, Abbottabad 22060, Pakistan

³ Present address: Department of Chemistry, King Faisal University, Al-Hasa, Saudi Arabia

Experimental

Instrumentation

^1H and ^{13}C NMR spectra were recorded on a Bruker Avance [300, 75.5 MHz] spectrometer. Chemical shifts are expressed in ppm with reference to TMS as internal standard. Mass spectra were obtained from a Micromass Zabtec or Finnigan MAT 95 XP instrument. Melting points were determined on an Electrothermal-9002 apparatus. IR spectra were recorded on a Varian IR-660 spectrometer. UV–vis spectra were measured on a Cary 5000 UV–vis–NIR (Varian) spectrometer. Fluorescence spectra were recorded on a modified version of Edinberg instruments spectrophotometer model FS-900SDT.

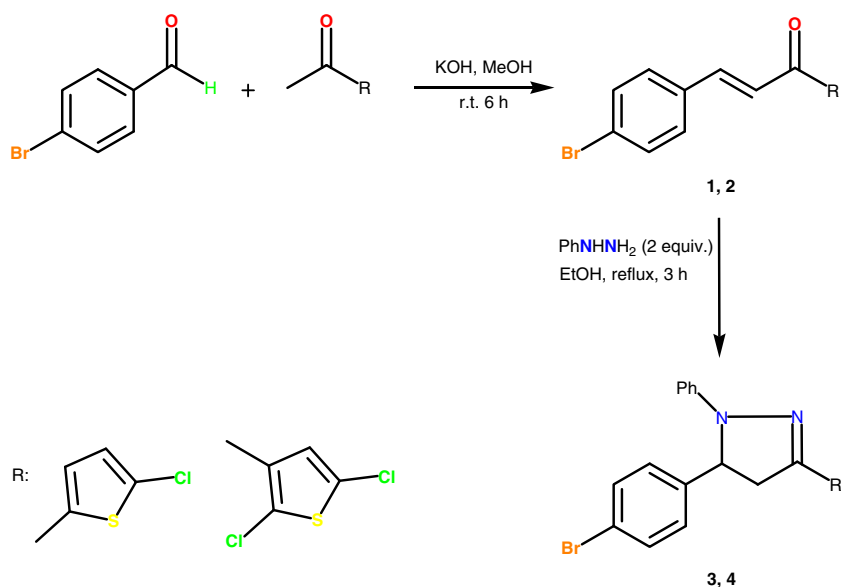
Materials

All the reagents were purchased from commercial suppliers and used without further purification. The phenylhydrazine, used in this study, were purchased from Sigma-Aldrich.

General Procedure for the Synthesis of Chalcones **1** and **2**

Chalcones **1** and **2** were prepared according to literature procedure [26]. A solution of the corresponding acetylthiophene (2.0 mmol) in MeOH (5.0 mL) was added dropwise to a solution containing the corresponding aldehyde (2.0 mmol) and KOH (4.0 mmol, 2 equiv.) in MeOH (20 mL). The reaction mixture was stirred for 6 h at room temperature until completion of the reaction. The precipitate formed was filtered off, washed with cold MeOH, and dried. The solid product was recrystallized from MeOH. The progress of all reactions was monitored by thin layer chromatography (TLC) (Scheme 1).

Scheme 1 Preparation of pyrazolines **3** and **4**



Synthesis and Characterization of Pyrazolines **3** and **4**

The pyrazolines **3** and **4**, Scheme 2, were prepared using the following general procedure:

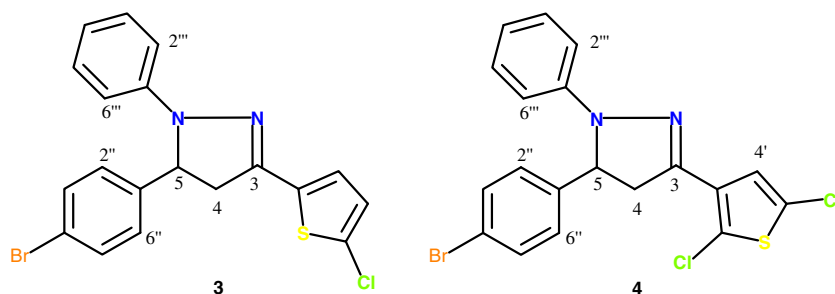
A mixture of appropriate chalcone (0.25 mmol) and phenylhydrazine (0.50 mmol, 2 equiv.) was dissolved in EtOH (25 mL) and refluxed for 3 h. The reaction mixture was allowed to cool, the precipitate formed, filtered off, dried and then recrystallized from EtOH.

The compounds **3** and **4** were characterized by IR and ^1H and ^{13}C NMR methods and selected results are given below:

5-(4-bromophenyl)-3-(5-chlorothiophen-2-yl)-1-phenyl-4,5-dihydro-1*H*-pyrazole (**3**): Pale-yellow solid, yield 57 %. m.p. 133–134 °C. IR (KBr, cm^{-1}): $\nu = 2914, 2360, 1595, 1495, 1319$. ^1H NMR (300 MHz, CDCl_3 , ppm): $\delta = 3.01$ (dd, $^2J_{4a,4b} = 16.9$ Hz, $^3J_{4a,5} = 7.2$ Hz, 1H, 4-Ha), 3.75 (dd, $^2J_{4a,4b} = 16.9$ Hz, $^3J_{4b,5} = 12.3$ Hz, 1H, 4-Hb), 5.20 (dd, $^3J_{4a,5} = 7.2$ Hz, $^3J_{4b,5} = 12.3$ Hz, 1H, 5-H), 6.73 (d, $^3J_{3',4'} = 3.9$ Hz, 1H, 3'-H), 6.79 (d, $^3J_{3',4'} = 3.9$ Hz, 1H, 4'-H), 6.80–6.83 (m, 1H, 4''-H), 6.95 (d, $^3J_{2'',3''} = ^3J_{5'',6''} = 7.7$ Hz, 2H, 2''-H, 6''-H), 7.13–7.18 (m, 4H, 2'''-H, 3'''-H, 5'''-H, 6'''-H), 7.45 (d, $^3J_{2'',3''} = ^3J_{5'',6''} = 8.4$ Hz, 2H, 3''-H, 5''-H). ^{13}C NMR (75.5 MHz, CDCl_3 , ppm): $\delta = 43.4, 64.1, 113.4, 121.6, 125.0, 126.4, 127.6, 129.0, 131.3, 132.4, 135.1, 141.0, 142.1, 144.1$. HRMS (ESI) Calc. for $\text{C}_{19}\text{H}_{14}\text{BrClN}_2\text{S}$: 415.97441; Found: 415.97349. Anal for $\text{C}_{19}\text{H}_{14}\text{BrClN}_2\text{S}$ (417.7 g/mol). Calc. C, 54.63 %; H, 3.38 %; N, 6.71 %; S, 7.67 %. Found: C, 55.08 %; H, 3.49 %; N, 6.42 %; S, 7.42 %.

5-(4-bromophenyl)-3-(2,5-dichlorothiophen-3-yl)-1-phenyl-4,5-dihydro-1*H*-pyrazole (**4**): Yellow solid, yield 63 %. m.p. 189–190 °C. IR (KBr, cm^{-1}): $\nu = 2358, 1594, 1485, 1329$. ^1H NMR (300 MHz, CDCl_3 , ppm): 3.23 (dd, $^2J_{4a,4b} = 17.6$ Hz, $^3J_{4a,5} = 7.3$ Hz, 1H, 4-Ha), 3.94 (dd, $^2J_{4a,4b} = 17.6$ Hz, $^3J_{4b,5} = 12.5$ Hz, 1H, 4-Hb),

Scheme 2 The structures of compounds **3** and **4** with atom numbering scheme



5.21 (dd, $^3J_{4a,5} = 7.3$ Hz, $^3J_{4b,5} = 12.5$ Hz, 1H, 5-H), 6.78 (t, $^3J_{3'',4'''} = ^3J_{4''',5'''} = 7.3$ Hz, 1H, 4'''-H), 6.95 (d, $^3J_{2'',3''} = ^3J_{5'',6''} = 8.8$ Hz, 2H, 2''-H, 6''-H), 7.13–7.19 (m, 4H, 2'''-H, 3'''-H, 5'''-H, 6'''-H), 7.33 (s, 1H, 4'-H), 7.44 (d, $^3J_{2',3'} = ^3J_{5',6'} = 8.4$ Hz, 2H, 3'-H, 5'-H). ^{13}C NMR (75.5 MHz, CDCl_3 , ppm): $\delta = 44.4, 64.1, 113.5, 119.8, 121.6, 123.1, 125.9, 126.9, 127.6, 129.0, 130.8, 132.4, 141.1, 141.5, 143.9$. HRMS (ESI) Calc. for $\text{C}_{19}\text{H}_{14}\text{BrCl}_2\text{N}_2\text{S}$: 450.94326; Found: 450.93217. Anal. for $\text{C}_{19}\text{H}_{13}\text{BrCl}_2\text{N}_2\text{S}$ (452.2). Calc. C, 50.47 %; H, 2.90 %; N, 6.20 %; S, 7.09 %. Found: C, 50.79 %; H, 2.93 %; N, 5.93 %; S, 7.10 %.

Computational Details

All calculations were performed with Gaussian 09 suite of programs [27]. Geometries were optimized without any symmetry constraints at hybrid B3LYP method using 6-31G (d,p) [28] basis set in the gas phase and in acetonitrile solvent. The B3LYP method consists of three parameter hybrid functional of Becke [29] in conjunction with the correlation functional of Lee, Yang, and Parr [30]. The B3LYP method provides a nice balance between cost and accuracy, and is known to perform very well for the prediction of geometries of a number of synthetic [31–34] and natural products [35, 36]. The optimized structures were confirmed by frequency analysis at the same level (B3LYP/6-31G(d,p)) as true minima (no imaginary frequency). The calculated frequencies are then scaled with a scaling factor of 0.9613. The UV-vis absorption spectrum was simulated using time dependant DFT method (TD-DFT) at B3LYP/6-31G(d,p) in acetonitrile solvent using IEFPCM model. For fluorescence, the excited states are optimized at TD-DFT method, and then, vertical energies are calculated while retaining the geometries of the excited states. ^1H and ^{13}C NMR calculations were performed at B3LYP/6-311 + G(2d,p) in chloroform solvent (CHCl_3) using GIAO formalism with TMS as internal standard. The electronic properties such as ionization potential, electron affinity, coefficient of highest occupied molecular orbital (HOMO), coefficient of lowest unoccupied molecular orbital (LUMO) and band gaps are also calculated at B3LYP/6-31G(d,P). The band gap is taken as the difference in energies of HOMO and LUMO.

Results and Discussion

Preparation of Pyrazoline Derivatives

Chalcones **1** and **2** (Scheme 1) were prepared by Claisen-Schmidt condensation of appropriate acetylthiophene with the corresponding aldehydes in presence of potassium hydroxide in methanol at room temperature [26]. Pyrazoline **3** and **4** derivatives were obtained in moderate yield by refluxing the appropriate chalcones (**1** and **2**) with two equivalents of phenylhydrazine for 3 h in ethanol (Scheme 1).

The products were characterized by HRMS (ESI), FT-IR, ^1H NMR, ^{13}C NMR and elemental analysis. The ^1H NMR spectra of compounds **3** and **4** displayed two *o*-coupled proton aromatic signals at δ 6.95 (d, 2''-H, 6''-H), 7.44 and 7.45 (d, 3''-H, 5''-H) supporting the presence of a 1,4-disubstituted benzene ring. In **3**, two doublets appeared at δ 6.73 (d, 3'-H), 6.79 (d, 4'-H), which are attributed to the thiophene protons, and it is clear from the small coupling constant (3.9 Hz). In compound **4**, one singlet appeared at δ 7.33 (s, 4'-H) corresponding to the thiophene proton. The aromatic proton 4'''-H appeared as triplet at δ 6.78 in compound **3**, while it appeared as a multiplet at δ 6.80–6.83 (m, 4'''-H) in **4**. The appearance of multiplets at δ 7.13–7.19 was due to the rest of aromatic protons in both compounds (m, 2'''-H, 3'''-H, 5'''-H, 6'''-H). Furthermore, a methine signal at δ 5.20 and 5.21 (dd, 5-H) for compounds **3** and **4**, respectively. An ABX system of a methylene group at δ 3.01 and 3.23 (dd, 4-Ha) for **3**, δ 3.75 and 3.94 (dd, 4-Hb) for **4**, were observed in the aliphatic region. ^{13}C NMR spectra displayed spectral signals that are in good agreement with the probable structures. ^{13}C NMR spectra for both compounds **3** and **4** showed a methine carbon signal at δ 64.1 (C-5), a methylene at δ 43.4 (C-4) [compound **3**], 44.4 (C-4) [compound **4**], as well as 13 sp^2 carbons in the range 113–145 [in both spectra for compound **3** and **4**].

The interpretation of the HRMS (ESI) data of compound **3** confirmed the molecular formula $\text{C}_{19}\text{H}_{14}\text{BrClN}_2\text{S}$ (m/z calc. 415.97441; Found 415.97349) implying 13 index of hydrogen deficiency; while the HRMS (ESI) (m/z calc. 450.94326; Found 450.93217) analysis data of compound **4** revealed the molecular formula $\text{C}_{19}\text{H}_{14}\text{BrCl}_2\text{N}_2\text{S}$.

Table 1 Selected geometric parameters of compound **3** in the gas phase and in MeCN (values in parenthesis), all bond lengths and angles are in Å and °, respectively

Atoms	Bond lengths (Å)	Atoms	Angle (°)
C-Br	1.91 (1.92)	N-N-C3	109.86 (109.68)
C5-C1''	1.52 (1.521)	N-C3-C2'	121.69 (121.62)
N-N	1.366 (1.366)	C5'-S-C2'	90.91 (90.81)
C3-C2'	1.446 (1.447)	S-C5'-Cl	120.48 (120.41)
C2'-S	1.758 (1.758)	Dihedral angles	
S-C5'	1.74 (1.742)	N-C5-C1''-C2''	34.57 (36.21)
C-Cl	1.73 (1.733)	N2-N1-C1'''-C2'''	7.00 (7.94)
		N2-C3-C2'-C3'	1.12 (1.46)

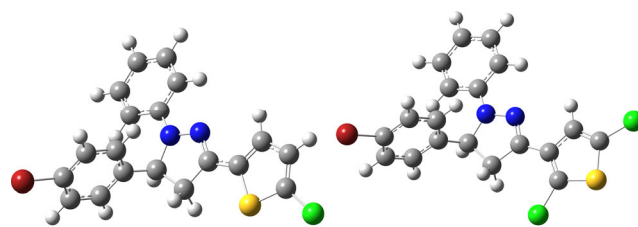
Optimized Geometries

The geometries were optimized at B3LYP/6-31G(d,p) level of theory, and important geometric parameters are given in Tables 1 and 2 for compounds **3** and **4**, respectively. The optimized geometries are shown in Fig. 1. A close look on the data reveals that most of the geometric parameters are very comparable for compounds **3** and **4**. The N-N bond length in the central ring is 1.366 Å for both compounds. Similarly, C5-1'' and C4''-Br bond lengths are 1.52 Å and 1.91 Å, respectively, for both compounds. Despite the above mentioned identical geometric parameters, some small differences are observed. For example, C3-C2' bond lengths are 1.446 Å and 1.456 Å for compounds **3** and **4**, respectively. The C2'-S and S-C5' bond lengths are a bit short for compound **4** compared to those in **3**.

Small differences in bond angles and dihedral angles are also observed in both compounds. For example, N-N-C3 bond angle is 109.86° in compound **3** which is slightly increased to 110.27° in compound **4**. However, the other bond angles such as N-C3-C2, C5-S-C2' and S-C5-Cl are decreased for compound **4** compared to those in **3**. The N-C3-C2, C5-S-C2' and S-C5-Cl bond angles are 121.69°, 90.91° and 120.48°, respectively for compound **3** which decrease to 119.68°, 89.82° and 120.09° for compound **4**.

Table 2 Selected geometric parameters of compound **4** in the gas phase and in acetonitrile (values in parenthesis), all bond lengths and angles are in Å and °, respectively

Atoms	Bond lengths (Å)	Atoms	Angle (°)
C-Br	1.91 (1.917)	N-N-C3	110.27 (110.07)
C5-C1''	1.52 (1.521)	N-C3-C3'	119.68 (119.68)
N-N	1.362 (1.363)	C5'-S-C2'	89.82 (89.78)
C3-C2'	1.456 (1.457)	S-C5'-Cl	120.09 (120.15)
C2'-S	1.747 (1.748)	Dihedral angles	
S-C5'	1.748 (1.748)	N-C5-C1''-C2''	34.91 (37.15)
C5'-Cl	1.730 (1.734)	N2-N1-C1'''-C2'''	8.83 (9.15)
C2'-Cl	1.736 (1.732)	N2-C3-C3'-C4'	0.74 (0.98)

**Fig. 1** Optimized molecular geometries of both compounds **3** (left) and **4** (right)

120.09° for compound **4**. The planarity of ring A with rings B, C and D is analyzed through dihedral angles N2-C3-C3'-C4', N-C5-C1''-C2'' and N2-N1-C1'''-C2''', respectively, for compound **3**. The ring B is almost co-planar with ring A, and the dihedral angle is 1.12°. The ring D makes an angle of 7.0° with ring A, but ring C is significantly bent away from planarity (34.57°). For compound **4**, these angles are 0.74, 8.83 and 34.91° for N2-C3-C3'-C4', N2-N1-C1'''-C2''' and N-C5-C1''-C2'', respectively.

Next, the geometries are optimized and analysed in acetonitrile solvent. The geometries in solvent are very comparable to those in gas phase. Bond lengths are almost identical whereas bond angles and dihedral angles are $\pm 1^\circ$.

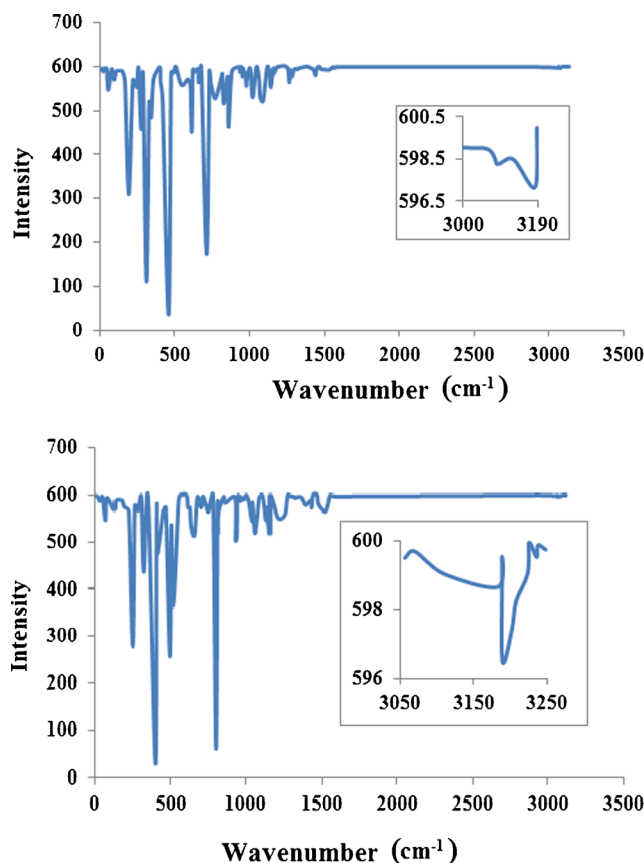
**Fig. 2** Theoretical IR spectrum of compound **3** (top) and **4** (bottom), calculated at B3LYP/6-31G(d,p)

Table 3 Comparative theoretical and experimental infra-red bands of compound **3**, and their approximate assignments

Sr. No	Vibration (Expt) cm^{-1}	Vibration Theor. Unscaled	Vibration Theor. Scaled	Approximate Assignment
1	2914	3270–3045	3135–2935	C-H str
2	1595	1652	1588	C = C str (Ar, ring D)
3	1560	1642	1579	C = C str (Ar, ring C)
4	1555	1620	1558	C = N str
5	1495	1539	1479	C-H bending
6	1475	1526	1467	C-H being (ring C)
7	1450	1484	1427	CH_2 bending
8	1381	1428	1373	C-H thiophene ring
9	1319	1373	1319	C-N bond str
10	1178	1234	1186	C-H ring B
11	632	663	637	Ar-Br

Infra-Red Analysis

Vibrational spectra of both compounds, Fig. 2, are studied theoretically and compared with the experiment. Important vibrational bands (scaled and unscaled) along with experimental bands are listed in Tables 3 and 4 for compounds **3** and **4**. In the functional group region of the spectrum, C-H stretching vibrations are calculated to appear at 3122–2938 cm^{-1} as compared to experimental which appears in the range 2358–2914 cm^{-1} .

Both compounds show very similar peaks in the functional group region of the vibrational spectrum, and this is expected due to their similar geometric parameters. The C = C and C = N stretching vibrations of the aromatic rings of both compounds appear in the range of 1500–1600 cm^{-1} . The C = C stretching vibration of the ring D of compounds **3** and **4** appears at 1588 cm^{-1} whereas the similar vibrations of the ring C are predicted at 1579 cm^{-1} . These C = C stretching vibrations correlate nicely with the experimental 1595 and 1594 cm^{-1} for compounds **3** and **4**, respectively. The C = N stretching vibration of compounds **3** and **4** appear at 1588 and 1553 cm^{-1} ,

which agree with the experimental 1555 and 1505 cm^{-1} vibrations, respectively.

The C-H bending vibrations for compounds **3** and **4** are experimentally observed at 1495 and 1485 cm^{-1} , respectively. In their theoretical spectrum, a number of peaks are observed in this region. For compound **3**, four prominent peaks are observed at 1479 (C-H bending of ring C), 1467 (C-H bending of ring D), 1427 (CH_2 bending of ring A) and 1373 cm^{-1} (C-H bending of ring B). The corresponding vibrations for compound **4** are 1477, 1468, 1428 and 1364 cm^{-1} . The C-N bond stretching vibrations for compounds **3** and **4** are calculated to appear at 1319 and 1314 cm^{-1} which again corroborate nicely with their experimental values at 1319 and 1329 cm^{-1} .

The UV-Vis Absorption and Fluorescence Emission Spectra

The UV-Vis spectra (Fig. 3) of the two pyrazolines **3** and **4** derivatives showed an intense absorption bands which may be attributed to the $\pi - \pi^*$ transition of the conjugated backbone [14, 37–39]. In case of absorption spectra of compounds **3** and

Table 4 Comparative theoretical and experimental infra-red bands of compound **4**, and their approximate assignments

Sr. No	Vibration (Expt) cm^{-1}	Vibration Theor. Unscaled	Vibration Theor. Scaled	Approximate Assignment
1	2358	3250–3050	3122–2938	C-H str
2	1594	1652	1588	C = C str (Ar, ring D)
3	1564	1642	1579	C = C str (Ar, ring C)
4	1505	1615	1553	C = N str
5	1485	1537	1477	C-H bending
6	1465	1527	1468	C-H being (ring C)
7	1407	1486	1428	CH_2 bending
8	1360	1418	1364	C-H thiophene ring
9	1329	1367	1314	C-N bond str
10	1120	1158	1113	C-H ring B
11	607	657	632	Ar-Br

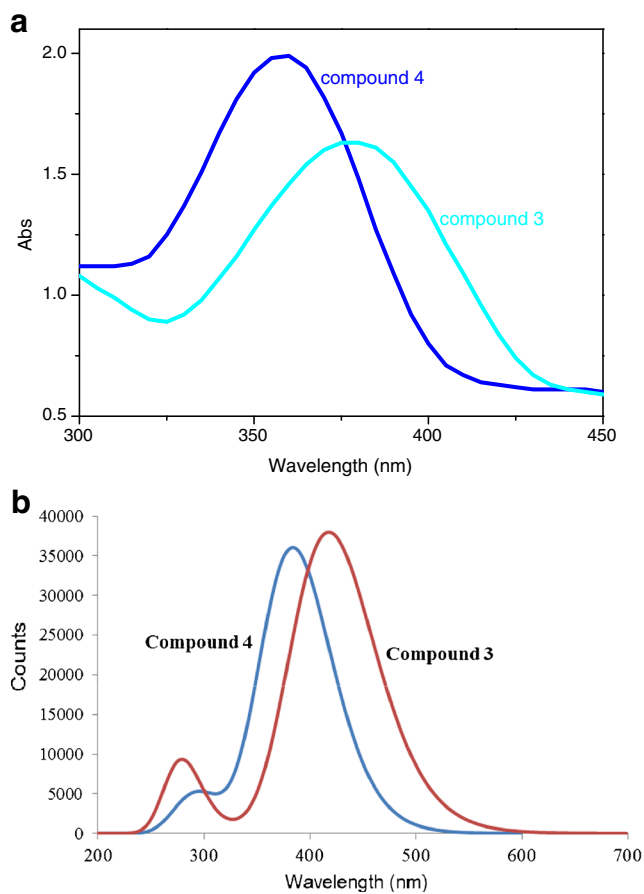


Fig. 3 The UV-Vis absorption spectra of **3** and **4**: (a) Experimental; (b) Theoretical

4, the absorption maxima ($\lambda_{\max}^{\text{abs}}$) wavelength was observed in the range of 360–380 nm (Table 5) with the corresponding absorbance. The difference of peak positions and intensity is due to the effect of the presence of different substituted thiophene groups at the 2-pyrazoline moiety.

The UV-Vis and emission spectroscopy was used to assess fluorescence properties of both pyrazoline derivatives. Compound **3** was found to be fluorescent (Fig. 4) and displayed fluorescence in the blue region of the visible spectrum (Fig. 5, Table 5), while **4** is not. The emission maxima ($\lambda_{\max}^{\text{em}}$) wavelengths of **3** lie in the blue region of visible spectrum and therefore show blue fluorescence.

Table 5 Absorption and fluorescence wavelengths of compounds **3** and **4**

Compound	Absorption (Ex*)	Absorption (Th*)	Emission (Ex*)	Emission (Th*)
3	380	418	560 (MeOH)	507
			572 (MeCN)	
			550 (hexane)	
4	360	278	No emission	460
		384		
		299		

*Th = theoretical; Ex = experimental

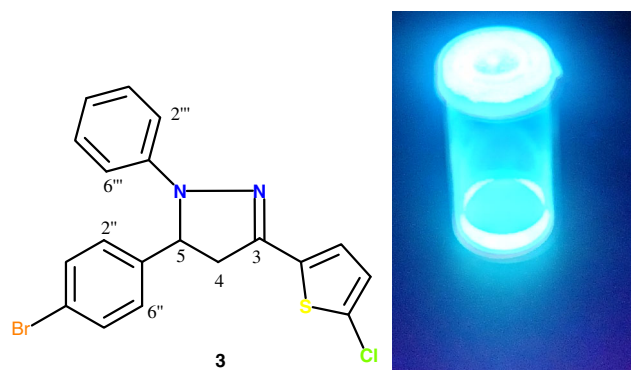


Fig. 4 Fluorescence of compound **3**

Density functional theory calculations have also been performed for absorption properties of these compounds. The absorption and emission spectrum are calculated using time dependent DFT calculations at B3LYP/6-31G(d,p). Compound **3** is calculated to absorb at 418 nm ($\lambda_{\max}^{\text{abs}}$) with an oscillator strength of 0.94. This absorption maximum is slightly higher than the experimental 380 nm. Similarly, the absorption maximum of compound **4** is also calculated relatively higher (384 nm) than the experimental 360 nm. The oscillator strength of the band at 384 nm for compound **4** is 0.89. For both compounds, relatively weak absorptions are also predicted between 270 and 300 nm. For compound **3**, these peaks appear at 286 and 278 nm with oscillator strengths of 0.03 and 0.19, respectively. For compound **4**, these peaks appear at 299 and 279 nm with oscillator strength of 0.09 and 0.05, respectively.

To get an estimate of the emission wavelengths, the geometries of both compounds are optimized in the excited states and then energy difference is taken between relaxed geometry of the excited state and single point energy of the same geometry in the ground state. The calculated emission wavelength for compound **3** is 507 nm whereas compound **4** is expected to emit at 460 nm. The compound **3** shows much more pronounced shift of the emission wavelength compared to the absorption wavelength, when compared with compound **4**. This is consistent with the experimental observation. However, the extent of shift predicted with theoretical methods is relatively less when compared with experimental results.

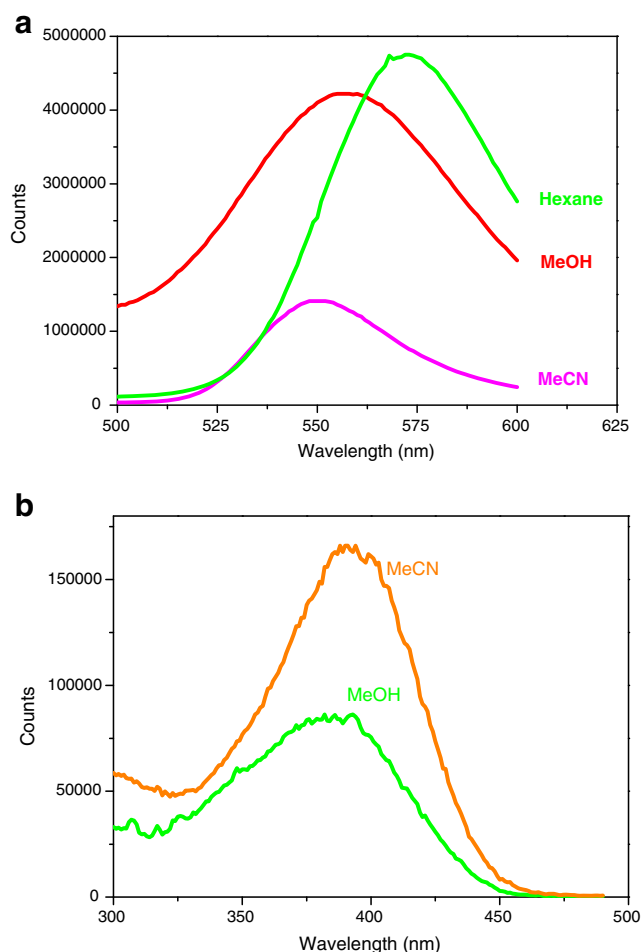


Fig. 5 Fluorescence emission spectra of: (a) **3** in different solvents (MeOH, MeCN and Hexane); (b) **4** in MeOH and MeCN

Frontier Molecular Orbital Analysis

Density functional calculations have been performed for frontier molecular orbitals to get insight into the electronic structures of both compounds. The frontier molecular orbitals of both compounds are shown in Fig. 6. The HOMOs of both compounds are very similar. They have density on the nitrogen atom of the central ring as well on the thiophene ring (ring B) and an aromatic ring (ring D). The HOMO is a π type orbital. Although the densities are very comparable but there is difference particularly regarding the density on the thiophene ring. In compound **3**, the density is distributed on the entire thiophene ring, however, only one double bond of the thiophene ring compound **3** is devoid of any electron density. This difference probably arises from the connectivity of the thiophene ring with the central ring (ring A). The HOMO of compound **3** has energy of -5.04 eV whereas the HOMO of compound **4** has -5.19 eV energy. The LUMO in both compounds is again π in nature however; the density is mainly located on the thiophene ring. The HOMO-LUMO gaps for compounds **3** and **4** are 3.46 and 3.73 eV respectively. The

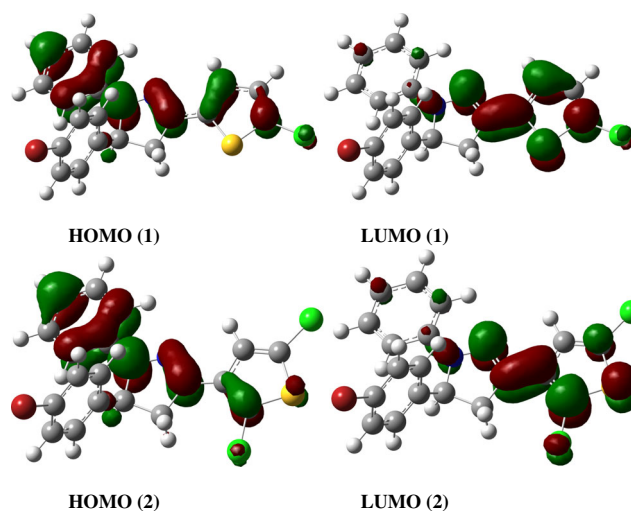


Fig. 6 Frontier molecular orbitals of compounds **3** (top) and **4** (bottom)

HOMO to LUMO transition is a charge transfer from the aromatic ring (ring D) to the thiophene ring (ring B). This transition is actually a π to π^* transition.

The Solvent Effect on Fluorescence Emission

The solvent effects on the fluorescence characteristics of compound **3** were also investigated. The emission wavelength of the compound **3** appears to be red-shifted in polar solvents compared to non-polar (Fig. 5 and Table 5).

Theoretical NMR Calculations

The NMR of the pyrazolines **3** and **4** are calculated at B3LYP/6-311 + G(2d,p) in chloroform solvent (PCM) through GIAO approach. Theoretical ^1H NMR chemical shifts are compared

Table 6 Theoretical and experimental ^1H NMR chemical shifts are compared for compounds **3** and **4**

	Comp 3 (Ex)	Comp 3(Th)	Comp 4 (Ex)	Comp 4 (Th)
H-4a	3.01	2.85	3.75	3.36
H-4b	3.23	3.9	3.94	4.28
H-5	5.20	5.39	5.21	5.46
H-3'	6.79	7.81	7.33	7.9
H-4'	6.73	7.15		
H2''	6.95	7.5	6.95	7.55
H3''	7.44	7.71	7.44	7.33
H5''	7.45	7.85	7.45	7.85
H6''	6.95	7.66	6.95	7.72
H2'''	7.13–7.19	6.51	7.13–7.19	6.47
H3'''	7.13–7.19	7.36	7.13–7.19	7.36
H4'''	7.13–7.19	7.01	7.13–7.19	7.07
H5'''	7.13–7.19	7.65	7.13–7.19	7.63
H6'''	7.13–7.19	8.11	7.13–7.19	8.1

with experimental chemical shifts for compounds **3** and **4**, and values are given in Table 6. The methane proton of the central ring (ring A) is calculated to appear at 5.39 for compound **3** which agrees very well with the experimental 5.20 ppm. The similar proton in compound **4** is calculated slightly downfield at 5.46 ppm which corroborates nicely with the experimental 5.21 ppm. The methylene proton of the ring A are calculated to appear at 2.85 and 3.9 ppm which are slightly different than the experimental 3.01 and 3.03 ppm for compound **3**. The corresponding methylene protons in compound **4** at 3.36 and 4.28 ppm correlate better with the experimental 3.75 and 3.94 ppm. The protons on the thiophene ring of compound **3** are calculated to appear at 7.81 and 7.15 for H-3' and H-4', respectively. These values are slightly overestimated but their trend agrees well with the experimental values of 6.79 and 6.73 ppm. The H-3' proton in compound **4**, however, agrees better with experimental 7.33 ppm. The other aromatic protons of rings C and D are calculated in the range of 6.5 to 8.1 ppm for both compounds compared to experimental 6.9–7.5 ppm.

Concluding Remarks

Two new pyrazoline derivatives were synthesized and characterized using spectral and microanalytical techniques. The molecular structures of both derivatives were optimized using DFT at B3LYP/6-31G(d,p) level of theory. The calculated UV-visible, fluorescence, IR spectra and ¹H NMR spectra for the optimized structures were found to agree well with experimental ones. The geometry of the pyrazoline derivatives has a configuration such that the different substituted thiophene groups at the 3-position is in conjugation with the central 2-pyrazoline ring. Therefore, it is expected to have significant effect on the properties of both derivatives (different electron donating ability). From emission spectra, it can be concluded that the introduction of different substituted thiophene at the 3-position strongly affects the emission properties and causing major shift in the emission wavelength.

Acknowledgments The authors are grateful to Al Al-Bayt University (Mafraq, Jordan) and the German Academic Exchange Service (DAAD) for financial support (Postdoctoral fellowship to Dr. Mohammad Ibrahim) and to Professor Dr. Svetlana Tsogoeva (Friedrich-Alexander-Universität Erlangen-Nürnberg/Germany) for her continuous support and valuable discussions. The authors would like also to thank Professor Idrees Al-Momani for his help in running the fluorescence emission spectra.

References

- Bano S, Alam MS, Javed K, Dudeja M, Das AK, Dhulap A (2015) Synthesis, biological evaluation and molecular docking of some substituted pyrazolines and isoxazolines as potential antimicrobial agents. *Eur J Med Chem* 95:96–103
- Lone I, Khan K, Fozdar B (2014) Synthesis, physicochemical properties, antimicrobial and antioxidant studies of pyrazoline derivatives bearing a pyridyl moiety. *Med Chem Res* 23:363–369
- Zhu S-L, Wu Y, Liu C-J, Wei C-Y, Tao J-C, Liu H-M (2013) Design and stereoselective synthesis of novel isosteviol-fused pyrazolines and pyrazoles as potential anticancer agents. *Eur J Med Chem* 65: 70–82
- Lv P-C, Li D-D, Li Q-S, Lu X, Xiao Z-P, Zhu H-L (2011) Synthesis, molecular docking and evaluation of thiazolyl-pyrazoline derivatives as EGFR TK inhibitors and potential anti-cancer agents. *Bioorg Med Chem Lett* 21:5374–5377
- Havrylyuk D, Kovach N, Zimenkovsky B, Vasylenko O, Lesyk R (2011) Synthesis and anticancer activity of isatin-based pyrazolines and thiazolidines conjugates. *Arch Pharm* 344:514–522
- Viveka S, Dinesha SP, Nagaraja GK, Ballav S, Kerkar S (2015) Design and synthesis of some new pyrazolyl-pyrazolines as potential anti-inflammatory, analgesic and antibacterial agents. *Eur J Med Chem* 101:442–451
- He J, Ma L, Wei Z, Zhu J, Peng F, Shao M, Lei L, He L, Tang M, He L, Wu Y, Chen L (2015) Synthesis and biological evaluation of novel pyrazoline derivatives as potent anti-inflammatory agents. *Bioorg Med Chem Lett* 25:2429–2433
- Bandgar BP, Adsul LK, Chavan HV, Jalde SS, Shringare SN, Shaikh R, Meshram RJ, Gacche RN, Masand V (2012) Synthesis, biological evaluation, and docking studies of 3-(substituted)-aryl-5-(9-methyl-3-carbazole)-1H-2-pyrazolines as potent anti-inflammatory and antioxidant agents. *Bioorg Med Chem Lett* 22: 5839–5844
- Taj T, Kamble RR, Gireesh TM, Hunnur RK, Margankop SB (2011) One-pot synthesis of pyrazoline derivatised carbazoles as antitubercular, anticancer agents, their DNA cleavage and antioxidant activities. *Eur J Med Chem* 46:4366–4373
- Özdemir Z, Kandilci HB, Gümüşel B, Çalış Ü, Bilgin AA (2007) Synthesis and studies on antidepressant and anticonvulsant activities of some 3-(2-furyl)-pyrazoline derivatives. *Eur J Med Chem* 42:373–379
- Rajendra Prasad Y, Lakshmana Rao A, Prasoona L, Murali K, Ravi Kumar P (2005) Synthesis and antidepressant activity of some 1,3,5-triphenyl-2-pyrazolines and 3-(2"-hydroxy naphthalen-1"-yl)-1,5-diphenyl-2-pyrazolines. *Bioorg Med Chem Lett* 15:5030–5034
- Kumar S, Bawa S, Drabu S, Kumar R, Gupta H (2009) Biological activities of pyrazoline derivatives - a recent development. *Recent Pat Antiinfect Drug Discov* 4:154–163
- Li JF, Guan B, Li DX, Dong C (2007) Study on the fluorescence properties of a new intramolecular charge transfer compound 1,5-diphenyl-3-(N-ethylcarbazole-3-yl)-2-pyrazoline. *Spectrochim Acta A* 68:404–408
- Abbas A, Hussain S, Hafēz N, Naseer MM (2014) Synthesis and spectral characterization of new homologous 1,3,5-triaryl-2-pyrazolines: influence of alkyloxy chain length on fluorescence. *Spectrochim Acta A* 133:182–189
- Lu B, Zhang J, Wang M, Zhou Y, Chen X (2012) Synthesis and fluorescent property of pyrazoline derivatives. *Chin J Chem* 30: 1345–1350
- Li M-M, Zhao W-B, Zhang T-T, Fan W-L, Xu Y, Xiao Y, Miao J-Y, Zhao B-X (2013) A new thiophenyl pyrazoline fluorescent probe for Cu²⁺ in aqueous solution and imaging in live cell. *J Fluoresc* 23: 1263–1269
- Bian B, Ji S-J, Shi H-B (2008) Synthesis and fluorescent property of some novel bischromophore compounds containing pyrazoline and naphthalimide groups. *Dyes Pigments* 76:348–352
- Lu Z, Jiang Q, Zhu W, Xie M, Hou Y, Chen X, Wang Z (2000) Novel pyrazoline derivative used as light emitter in blue organic electroluminescent devices. *Synth Met* 111:465–468
- Wang P, Onozawa-Komatsuzaki N, Himeda Y, Sugihara H, Arakawa H, Kasuga K (2001) 3-(2-Pyridyl)-2-pyrazoline

- derivatives: novel fluorescent probes for Zn^{2+} ion. *Tetrahedron Lett* 42:9199–9201
20. Wilkinson F, Kelly GP, Michael C, Oelkrug D (1990) A study of the photophysical properties of various triaryl-2-pyrazolines in solution and microcrystalline form. *J Photochem Photobiol A Chem* 52: 309–320
 21. Tasch S, Niko A, Leising G, Scherf U (1996) Highly efficient electroluminescence of new wide band gap ladder-type poly (paraphenylenes). *Appl Phys Lett* 68:1090–1092
 22. Susan F (2000) Organic electroluminescent devices: enhanced carrier injection using SAM derivatized ITO electrodes. *J Mater Chem* 10:169–173
 23. Xiao D, Xi L, Yang W, Fu H, Shuai Z, Fang Y, Yao J (2003) Size-tunable emission from 1, 3-diphenyl-5-(2-anthryl)-2-pyrazoline nanoparticles. *J Am Chem Soc* 125:6740–6745
 24. Poteau X, Brown AI, Brown RG, Holmes C, Matthew D (2000) Fluorescence switching in 4-amino-1, 8-naphthalimides: “on–off–on” operation controlled by solvent and cations. *Dyes Pigments* 47:91–105
 25. Shi H-B, Ji S-J, Bian B (2007) Studies on transition metal ions recognition properties of 1-(2-benzothiazole)-3-(2-thiophene)-2-pyrazoline derivatives. *Dyes Pigments* 73:394–396
 26. Ibrahim MM (2015) Synthesis and characterization of new 3,5-disubstituted-4,5-dihydro-1H-pyrazole and their carbothioamide derivatives. *Eur J Chem* 6:78–83
 27. Frisch M, Trucks G, Schlegel H, Scuseria G, Robb M, Cheeseman J, Scalmani G, Barone V, Mennucci B, Petersson G, Nakatsuji H, Caricato M, Li X, Hratchian H, Izmaylov A, Bloino J, Zheng G, Sonnenberg JL, Had M (2010) Gaussian 09, in: Gaussian Inc
 28. Hariharan PC, Pople JA (1973) The influence of polarization functions on molecular orbital hydrogenation energies. *Theor Chim Acta* 28:213–222
 29. Becke AD (1993) Density-functional thermochemistry. III The role of exact exchange. *J Chem Phys* 98:5648–5652
 30. Lee C, Yang W, Parr RG (1988) Development of the Colle-Salvetti correlation-energy formula into a functional of the electron density. *Phys Rev B* 37:785–789
 31. Ullah H, Shah A-u-HA, Ayub K, Bilal S (2013) Density functional theory study of poly (o-phenylenediamine) oligomers. *J Phys Chem C* 117:4069–4078
 32. Javed I, Khurshid A, Arshad MN, Wang Y (2014) Photophysical and electrochemical properties and temperature dependent geometrical isomerism in alkyl quinacridonediimines. *New J Chem* 38: 752–761
 33. Babar A, Khalid H, Ayub K, Saleem S, Waseem A, Mahmood T, Munawar MA, Abbas G, Khan AF (2014) Synthesis, characterization and density functional theory study of some new 2-anilinothiazoles. *J Mol Struct* 1072:221–227
 34. Hung TQ, Thang NN, Dang TT, Ayub K, Villinger A, Friedrich A, Lochbrunner S, Flechsig G-U, Langer P (2014) Palladium catalyzed synthesis and physical properties of indolo [2, 3-b] quinoxalines. *Org Biomol Chem* 12:6151–6166
 35. Hashmi MA, Khan A, Ayub K, Farooq U (2014) Spectroscopic and density functional theory studies of 5, 7, 3', 5'-tetrahydroxyflavanone from the leaves of *Olea ferruginea*. *Spectrochim Acta A* 128: 225–230
 36. Ullah H, Rauf A, Ullah Z, Anwar M, Uddin G, Ayub K (2014) Density functional theory and phytochemical study of pistagremic acid. *Spectrochim Acta A* 118:210–214
 37. Liu W, Wang Y, Sun M, Zhang D, Zheng M, Yang W (2013) Alkoxy-position effects on piezofluorochromism and aggregation-induced emission of 9, 10-bis(alkoxystyryl)anthracenes. *Chem Commun* 49:6042–6044
 38. Khosa MA, Shah SS, Nazar MF (2011) UV-visible spectrometric study and micellar enhanced ultrafiltration of alizarin red S dye. *J Dispers Sci Technol* 32:1634–1640
 39. Hasan A, Abbas A, Akhtar MN (2011) Synthesis, characterization and fluorescent property evaluation of 1, 3, 5-triaryl-2-pyrazolines. *Molecules* 16:7789–7802